A 28 dBm-EIRP low-profile D-band transmitting module with a folded transmitarray antenna

Francesco Foglia Manzillo, Abdelaziz Hamani, Alexandre Siligaris, Antonio Clemente, José Luis Gonzalez Jimenez

A 28 dBm-EIRP Low-Profile D-band Transmitting Module with a Folded Transmitarray Antenna

F. Foglia Manzillo, A. Hamani, A. Siligaris, A. Clemente, and J. L. González-Jiménez
CEA-Leti, Univ. Grenoble Alpes, F-38000 Grenoble, France
{francesco.fogliamanzillo, joseluis.gonzalezjimenez}@cea.fr

***Abstract*— This work presents the design and characterization of a high-gain transmitting module including a two-channel 45-nm CMOS transmitter and a folded transmitarray antenna. The proposed architecture enables the reduction by a factor three of the antenna height and a significant enhancement of the efficiency with respect to similar state-of-art D-band modules. The performance of this compact design is compared to that of an equivalent system with a standard transmitarray antenna, driven by the same integrated circuit. The experiments prove that the folded transmitarray preserves the effective isotropic radiated power (28 dBm at 148 GHz) achieved by the bulkier standard transmitarray, over the operating band of the integrated circuit, spanning from 139.3 GHz to 156.6 GHz.**

***Keywords*— CMOS, millimeter-wave circuits, millimeter-wave antennas, antennas-in-package, active antennas, lens antennas.**

I. Introduction

Sub-THz transmitting modules for short-range communications or imaging systems require a very high effective isotropic radiated power (EIRP) and energy efficiency over relatively large fractional bandwidths. Moreover, they have to be realized using low-cost fabrication technologies to enable their massive deployment in ultra-dense networks. High EIRP values are often obtained using phased arrays that require a radiofrequency (RF) chain for each radiating element or small clusters of elements. Thus, they are limited by their poor scalability, low efficiency and high power consumption [1], [2].

Architectures based on lenses fed by small focal-plane antennas connected to a single transmitter (TX) [3]-[6] offer a more efficient solution for achieving a high antenna gain at sub-THz frequencies. However, the use of dielectric lenses generally leads to electrically large and lossy antennas [3], [4]. The primary sources are often inefficient on-chip antennas, while the lenses are fabricated with different processes, such as silicon micromachining [3] or additive manufacturing [4].

A few D-band TX modules based on low-loss flat lenses, or transmitarray antennas (TAs), have been recently demonstrated in [5], [6]. These TXs perform channel bonding to enhance the energy efficiency and relax the specifications on the design of the integrated circuit (IC), in terms of fractional bandwidth and operating frequency throughout the up-conversion chain, from baseband to RF. Flat lenses and feeds were realized in two standard printed circuit boards (PCBs). The overall heights of these modules (~30 mm) hinder their monolithic integration.

This paper presents a novel low-profile high-directivity D-band antenna module, based on a folded TA architecture [7]. The two-channel 45-nm CMOS TX IC described in [8] feeds two antennas on a PCB with signals laying in adjacent sub-bands. These primary antenna sources illuminate a large flat lens, also realized in low-cost PCB technology. The two signals emitted by the IC are aggregated over the air, thanks to a proper design of the lens. This new channel-bonding approach significantly enhances the EIRP, as it does not require guided power combiners, which at D-band may introduce high insertion losses, e.g. ~10 dB in [5]. In an 11.7%-fractional bandwidth, the measured EIRP of the proposed module is comparable to that of a second prototype, three times thicker, based on a standard TA architecture, which comprises the same lens and a very similar feed. To the best of the authors' knowledge, this is the first report of an active folded TA module. Moreover, the performance of a folded TA is compared for the first time at D-band with that of a conventional TA design.

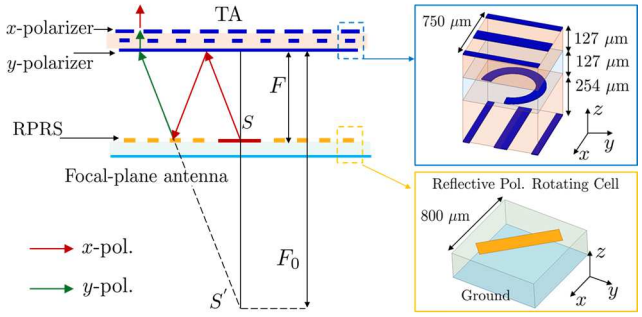

Fig. 1. Overview and principle of operation of the proposed folded TA.

II. Low-Profile Transmitarray Design and Integration

A. Overview of the folded transmitarray system

The folded TA comprises two PCBs: a primary antenna source fed by the TX IC presented in [8], which radiates an *x*-polarized field, and a flat discrete lens, at a distance *F*. The antenna elements of the source are surrounded by a reflective polarization-rotating surface (RPRS). It effectively converts an incident *x*-polarized field into a reflected *y*-polarized one. The bianisotropic unit-cells (UCs) of the lens are based on the designs in [6], [7]. The bottom and outer metal layers of the lens realize orthogonal wire grid polarizers. Thus, the *x*-polarized field emitted by the primary source is reflected by the lens. Then, the field is rotated by 90° and reflected back by the RPRS. Eventually, this *y*-polarized field is transmitted to the lens, which radiates an *x*-polarized field, as schematically shown in Fig. 1. Within the assumptions of geometrical optics and considering a perfect RPRS, the folded TA is equivalent to a standard TA excited by the same source, rotated by 90° and placed in a virtual focus at a distance $F_0 = 3F$ from the lens [7].

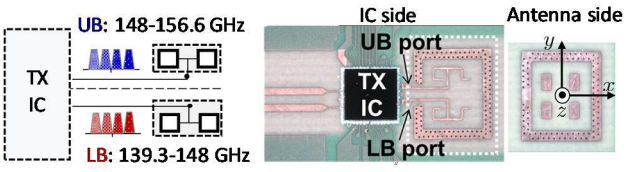

Fig. 2. Architecture and photograph of the focal-plane antenna module.

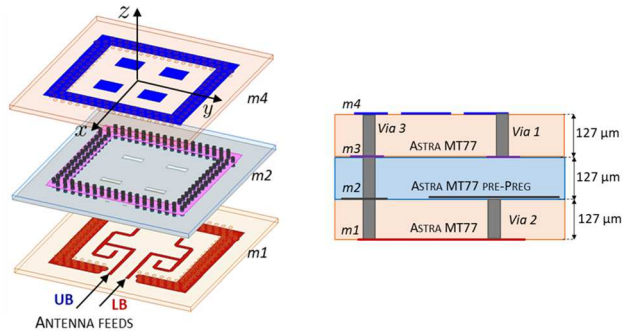

Fig. 3. Exploded view and stack-up of the focal-plane antenna module.

A. Focal-plane antenna module

The primary source of the TA is a two-port antenna, excited by the two outputs of the TX IC. The IC is designed to provide a multi-channel modulated signal in the band from 139.3 GHz to 156.6 GHz. This frequency range is covered using two output signals, each one spanning over half this bandwidth, namely the lower band (LB) and the upper band (UB). Each IC output is connected to an antenna source, as schematically shown in Fig. 2. Each antenna input line excites two aperture-coupled patches, parallel-fed by a microstrip power divider. The full-band signal is obtained by over-the-air power combination, performed by the TA, of the LB and UB signals radiated by the corresponding antennas. This solution avoids the use of lossy power combiners [5], [6] to output a single wideband signal.

The IC is flip-chipped on the backside of the low-cost four-layer PCB (Isola Astra MT77) embedding the patch antennas and related feed networks. The stack-up is shown in Fig. 3. The antenna elements are on the layer *m4*. The center-to-center distance between the two patch arrays, along the *y*-axis, and that between the two patches in each array (*x*-axis), are both 1.25 mm. The patches are excited by microstrip lines on *m1,* through rectangular slots in the ground plane on *m2*. A 3.3mm×2.9mm cavity around the patches is realized with through-hole vias (*via3* in Fig. 3). It suppresses surface-wave modes. The phase centers of LB and UB patch arrays are offset with respect to the *x*-axis. Therefore, the H-plane (*yz*-plane) cuts of the radiation patterns of the LB and UB arrays are tilted. For instance, the simulated realized gain patterns at 148 GHz (see Fig. 4), obtained using Ansys Electronics Desktop 2022, exhibit a maximum at ±18°, for LB and UB array, respectively, and a boresight gain of 7.7 dBi, i.e. 1.1 dB less than the peak value.

Two focal-plane antenna modules, shown in Fig. 5, were fabricated for illuminating the proposed folded TA and the corresponding standard TA, respectively, and to compare their performance. They differ only for the presence, in the folded

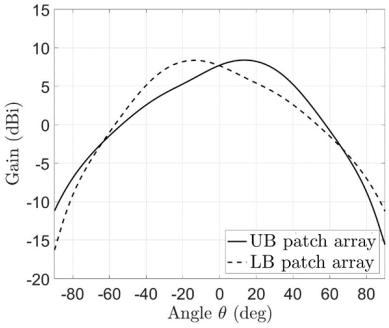

Fig. 4. Realized gain patterns (*yz*-plane cuts) of the focal-plane antenna of Fig. 2, when fed by either the LB or the UB input line at 148 GHz.

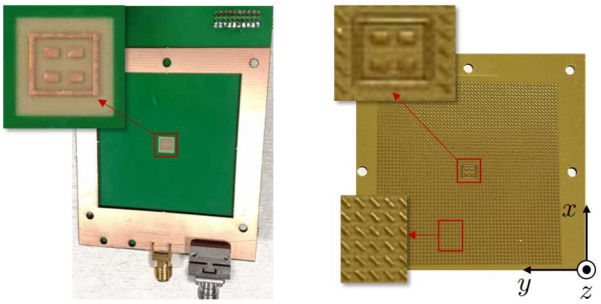

(a) (b)

Fig. 5. Pictures of the focal-plane modules used for the: (a) standard TA and (b) folded TA comprising a reflective polarization-rotating surface.

TA module, of an RPRS around the antennas, which converts an incident *x*-polarized plane wave into a reflected *y*-polarized one. The period of the RPRS is 0.8 mm, along both *x*- and *y*-axis. The RPRS UC comprises a rectangular strip, on *m4*, oriented at 45°, over the ground plane in *m2* (see the inset in Fig. 1). The simulated reflection coefficients (from *x*- to *y*-polarization) of the UC for a plane wave impinging at boresight and at 45° are greater than -0.2 dB and -1.2 dB, respectively, from 120 GHz to 160 GHz.

B. Transmitarray design and integration

The same planar lens is realized for the folded and the standard TA modules. As in [6], [7], the UCs of the lens are designed as three-layer asymmetric linear polarizers. All UCs comprise orthogonal wire grid polarizers on the outer layers. The element on the inner layer is designed to efficiently rotate by 90° the incident field and achieve a desired phase shift. The stack-up is shown in Fig. 1. Sixteen UCs were optimized using split rings and I-shaped patches. Simulations of the UCs under normal incidence in an infinite array environment confirm that an almost uniform 4-bit quantization of the 2π phase range is achieved between 125 GHz and 160 GHz (see Fig. 6a). The insertion loss in this frequency range is < 0.8 dB.

A 48×48 TA was designed to achieve a boresight gain higher than 25 dBi. Its electrical size is $17.8\lambda_0 \times 17.8\lambda_0$, where λ_0 is the free-space wavelength at 148 GHz, i.e. the frequency at the edge between LB and UB. The phase profile of the lens was determined using ray tracing at 148 GHz, assuming that the phase center of the primary source is aligned to the lens center,

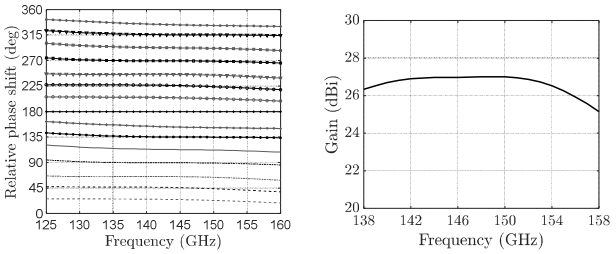

Fig. 6. (a) Simulated relative phase shifts introduced by 15 TA UCs with respect to a reference UC. (b) Computed gain of the standard TA module.

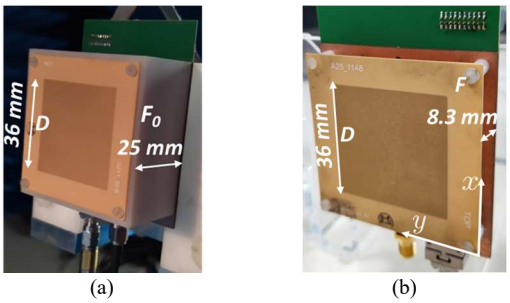

Fig. 7. (a) Standard TA module and (b) folded TA antenna module.

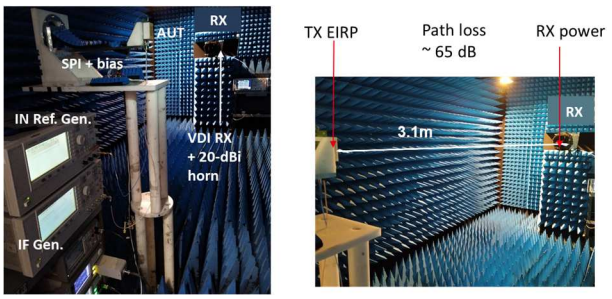

Fig. 8. Pictures of the setup used to characterize the antenna modules.

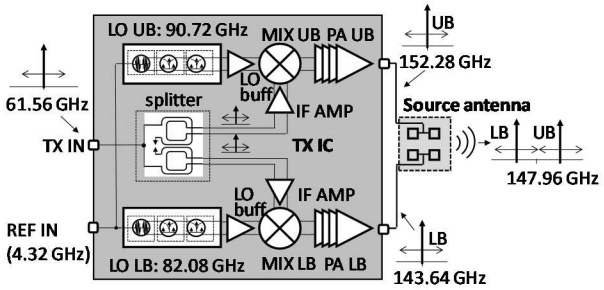

Fig. 9. Block diagram of the TX IC.

at a distance F_0. The lens size and F_0 were optimized, for the standard TA configuration, with the aid of a numerical tool based on the model described in [9]. This tool uses GO, the simulated far field of the focal-plane antenna and the scattering parameters of the lens UCs, to calculate the TA gain and radiation pattern versus frequency. Due to the off-focus position of the LB and UB patch arrays, the TA beam slightly tilts from boresight. The computed boresight gain for the standard TA is 27 dBi at 148 GHz and varies less than 1 dB in the 138-156-GHz band (see Fig. 6b). The difference between peak and boresight gain values at 148 GHz is 1.6 dB. Two samples of the designed lens are assembled on the focal-plane antenna boards, using plastic spacers, as shown in Fig. 7. The lens in the standard TA is rotated by 90°, with respect to that in the folded TA, to enable direct transmission. The flat lens in the folded TA is at a distance $F = F_0/3 = 8.3$ mm from the source. It is worth noting that, at this distance, the lens is not in far-field region of the source, as opposed to that in the standard TA.

III. Experimental Results

A. Measurement setup

The EIRP and radiation patterns of the two antenna systems were characterized in an anechoic chamber, at the output 1-dB compression point of the TX IC. The antenna under test (AUT) was mounted on a two-axis positioner. A receiver (RX) comprising a 20-dBi D-band horn and a commercial down-converter (VDI-SAX) was placed at 3.1 m from the AUT. The measurement setup and the instruments used to control and drive the TX modules are shown in Fig. 8. The TX IC feeding the focal-plane antenna comprises two up-conversion lanes, which are excited, for simplicity, by the same V-band signal at the input TX IN, as shown in Fig. 9. The LB and UB lanes have dedicated internal local oscillator (LO) generators, which provide LO signals at 82.08 GHz and 90.72 GHz, respectively. Therefore, when the IC is fed by a single-tone at TX IN, each up-conversion lane delivers, at the corresponding IC output, a tone in the LB and in the UB, respectively. In this way, the IC excites the focal-plane antenna with a two-tone signal, which is radiated by the LB and UB patch arrays, and eventually recombined by the TA.

The AUTs were characterized by sweeping the frequency of the tone at TX IN, so that their performance at the corresponding tones in the LB and UB could be measured simultaneously, using a spectrum analyzer connected to the RX. The RX power was measured as a function of frequency and elevation angle in the principal planes (*xz*- and *yz*-plane) of the AUT. The EIRP was obtained from these measurements after subtracting the RX gain and the path loss (~65 dB at 140 GHz).

B. Experimental results and discussion

First, the radiation patterns of the standard and folded TA modules are compared. The measured *xz*-plane cuts at the center frequencies of the LB and UB, obtained for an input tone at 61.56 GHz, are plotted in Fig. 10. As expected, the patterns of both AUTs are maximum at boresight. They are normalized to the boresight power received at 143.58 GHz. Indeed, the power emitted by TX IC in the LB is, in average, 3 dB higher than in the UB. The differences between the received power values at the two frequencies are 3 dB, for the standard TA (see Fig. 10a), and 1.8 dB, for the folded TA (see Fig. 10b). This 1.2-dB spread can be attributed to the variability of the fabrication and assembly processes of the ICs in the two modules, rather than to their different antenna architectures. The radiation patterns of the folded TA are overall similar to those of the standard TA, till the first sidelobes. However, they

exhibit a slightly narrower beamwidth and higher sidelobe levels (SLLs) for large elevation angles. These characteristics might be explained with near-field coupling effects between the source and the planar lens, as well as to a different aperture field distribution on the lens due to the angular-dependent reflection coefficient of the RPRS. The *yz*-plane patterns are shown in Fig. 11. Since the centers of the LB and UB patch arrays are offset with respect to the *x*-axis, the antenna beam tilts toward negative angles in the LB, and toward positive angles in the UB. The angular distance of the peaks of the beams at the two frequencies is 2°, for both TAs. The measured boresight gain is ~1.2 dB lower than the peak gain. This drop is consistent with that observed for the primary source in Fig. 3.

The measured EIRP values of the two modules, at boresight, are compared in Fig. 12, between 138 GHz and 158 GHz. The frequency behavior, including the dips around 148 GHz, i.e. at the edge between the LB and the UB, is mostly determined by the TX IC gain response. Indeed, both the focal plane and the TA antennas exhibit a quite flat gain in this frequency range (see Fig. 6b). Therefore, the 3-dB EIRP bandwidth is limited by the IC and could be extended using a larger number of channels, covering other sub-bands. Overall, the EIRP of the folded TA module is similar to that of the standard TA, in terms of bandwidth and absolute values. The shift towards higher frequencies (~2 GHz) of the response of the folded TA, with respect to that of the standard TA, is due, in part, to the variability of the IC assembly process. Indeed, the deformations of the C4 micro-bumps used to flip-chip the IC on the PCB are likely to change from sample to sample, thus affecting in different manners, in the two modules, the matching between the output ports of the IC and the focal-plane antenna. It is worth to observe that the over-the-air recombination of LB and UB signals enables a higher EIRP with respect to similar modules limited by the losses (~10 dB in [5]) of guided components performing channel aggregation.

IV. Conclusion

The design and characterization of two D-band TX modules with folded and conventional TAs have been presented. Both modules use an antenna-in-package fed by a two-channel 45-nm CMOS IC to illuminate the same flat lens, realized in PCB. The lens feeds differ only for the presence of a reflective polarization-rotating surface in the folded TA. Both modules radiate a signal spanning from 139.3 GHz to 156.6 GHz, by aggregating two sub-band signals emitted by the IC over the air, i.e. without using lossy power combiners. The folded TA attains an EIRP (28 dBm in average) very similar to that of the standard TA system, which is three times thicker. In the folded TA, the distance between the source and the lens is only 8.3 mm, which paves the way for the realization of monolithic high-gain sub-THz antenna modules in low-cost planar technologies.

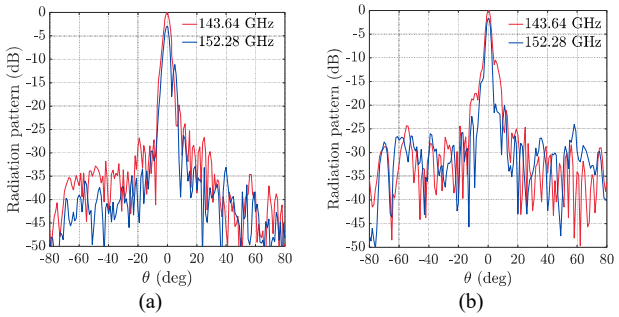

Fig. 10. Measured radiation patterns (*xz*-plane cut) of the (a) standard TA, and (b) folded TA modules, at the center frequencies of the LB and UB.

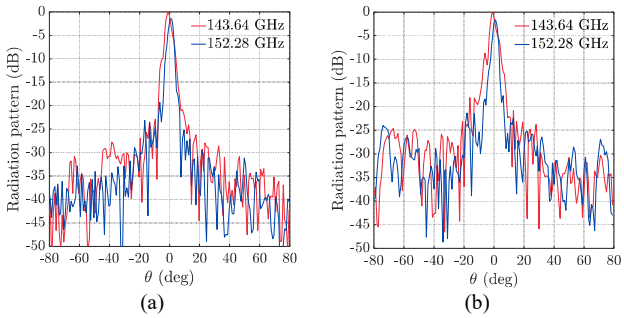

Fig. 11. Measured radiation patterns (*xz*-plane cut) of the (a) standard TA, and (b) folded TA modules, at the center frequencies of the LB and UB.

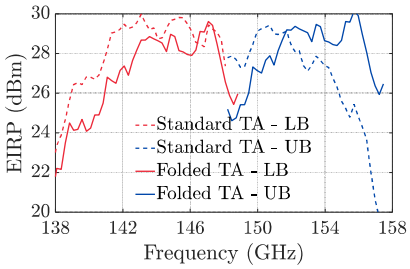

Fig.12. Measured EIRP at boresight ($\theta = 0^{o}$) for the two TAs (standard and folded) over the entire frequency range (LB and UB).

References

[1] D. del Rio *et al*., "A D-band 16-element phased-array transceiver in 55-nm BiCMOS," *IEEE Trans. Microw. Theory Techn.* 2022.

[2] S. Li, *et al*., "An eight-element 136–147 GHz wafer-scale phased-array transmitter with 32 dBm Peak EIRP and >16 Gbps 16QAM and 64QAM operation," *IEEE J. Solid-State Circ.*, vol. 57, no. 6, pp. 1635-1648, 2022.

[3] R. Han *et al*., "A SiGe terahertz heterodyne imaging transmitter with 3.3 mW radiated power and fully-integrated phase-locked loop," *IEEE J. Solid-State Circ.*, vol. 50, no. 12, pp. 2935–2947, 2015.

[4] B. Sene, D. Reiter, H. Knapp and N. Pohl, "Design of a cost-efficient monostatic radar sensor with antenna on chip and lens in package," *IEEE Trans. Microw. Theory Techn.*, vol. 70, no. 1, pp. 502-512, Jan. 2022.

[5] A. Hamani *et al*., "A D-Band multichannel TX system-in-package achieving 84.48 Gb/s with 64-QAM based on 45-nm CMOS and low-cost PCB technology," *IEEE Trans. Microw. Theory Techn.*, vol. 70, no. 7, pp. 3385-3395, 2022.

[6] J. L. Gonzalez-Jimenez, *et al*., "A D-band high-gain antenna module combining an in-package active feed and a flat discrete lens," in *Proc. 52nd Eur. Microw. Conf. (EuMC)*, pp. 784-787, Sept. 2022.

[7] Y. Ge et *al*., "Broadband folded transmitarray antenna based on an ultrathin transmission polarizer," *IEEE Trans. Antennas Propag.*, vol. 66, no. 11, 2018.

[8] A. Hamani *et al*., "A 56.32 Gb/s 16-QAM D-band wireless link using RX-TX systems-in-package with integrated multi-LO generators in 45nm RFSOI," *Proc. IEEE Radio Freq. Integr. Circ. Symp.* pp. 75-78, June 2022.

[9] H. Kaouach, *et al*., "Wideband low-loss linear and circular polarization transmit-arrays in V-band," *IEEE Trans. Antennas Propag.*, vol. 59, no. 7, pp. 2513–2523, 2011.